ARTICLES

Optical properties and electronic structures of equiatomic XTi (X=Fe, Co, and Ni) alloys

Joo Yull Rhee
Department of Physics, College of Natural Sciences, Hoseo University, Asan, Choongnam 336-795, Korea

B. N. Harmon and D. W. Lynch
Ames Laboratory–U.S. Department of Energy and Department of Physics and Astronomy, Iowa State University, Ames, Iowa 50011
(Received 8 February 1996)

The dielectric functions of equiatomic XTi (X=Fe, Co, and Ni) alloys in the $B2$ phase (cubic CsCl structure) were measured by spectroscopic ellipsometry in the energy range of 1.5–5.4 eV. The optical conductivity spectra show close resemblance to each other with a peak at 1.9–2.3 eV and another at 3.1–3.4 eV. Fine structures observed in previously reported measurements were not seen. The band structures and the optical conductivity spectra were calculated in the $B2$ phase using the linearized-augmented-plane-wave method with the local density approximation. The agreement between the measured and calculated spectra is markedly improved by the inclusion of a quasiparticle self-energy correction. Strong optical transitions are identified and the similarities and differences among the optical conductivity spectra of the three compounds are explained. [S0163-1829(96)01247-7]

At room temperature equiatomic FeTi and CoTi alloys have the cubic CsCl structure ($B2$ phase) and the equiatomic NiTi alloy has a monoclinic structure ($B19'$ phase). FeTi forms a very stable $B2$ phase at room temperature and CoTi is less stable than FeTi, while NiTi is unstable, undergoing a martensitic transformation[1] from the austenitic $B2$ phase at high temperature ($\geqslant$333 K) to the martensitic $B19'$ phase upon cooling. This transition is responsible for the so-called shape-memory effect.[2] CoTi and FeTi do not show such a transformation.

FeTi and CoTi alloys have stoichiometry-dependent magnetic properties. Both intermetallic compounds are paramagnetic and they form a continuous series of solid solutions. Pseudobinary $Fe_{1-x}Co_xTi$ alloys in the range $0.15 \leqslant x \leqslant 0.65$, are weakly ferromagnetic with $T_c \leqslant 70$ K.[3,4] However the origin of their magnetic moments is not clearly resolved, whether it is weakly itinerant,[5] governed by clusters, or by atoms located at antiphase boundaries,[6] or individual Fe and/or Co atoms placed on Ti sites.

These intriguing properties stimulated a number of experimental and theoretical studies. Especially investigations of the electronic structures and related properties were carried out and many experimental studies were performed on magnetic properties,[3,4] isomer shift measurements,[8] soft x-ray absorption and emission spectra, near-edge x-ray absorption spectra,[9] photoemission spectroscopy,[10,11] specific heat,[12] Hall coefficient,[13] and optical properties.[14–17] The de Haas–van Alphen effect was measured only for FeTi.[18]

The electronic structures were calculated for FeTi,[19–23] CoTi,[19,20] and NiTi (Refs. 19, 20, and 24–26) in the $B2$ phase. In Ref. 20 it was shown that the band structures and the density of states (DOS) of the three compounds are qualitatively similar to each other. The DOS curves have a deep minimum near the Fermi level, separating the higher bands, which have predominantly Ti d character with small Fe, Co, or Ni $3d$ character, and the lower bands, dominated by Fe, Co, or Ni d character with an admixture of Ti d character. The Fermi level moves from the minimum (FeTi) to the first maximum of the higher, unoccupied d bands (NiTi). The structural stability and the covalency of the compounds were explained by the location of the Fermi level.[20]

Zhao and Harmon[26] investigated the instability of the NiTi compound by calculating the electronic structure using a first-principles linear-combination-of-atomic-orbital method. They fitted the resulting band structure with a nonorthogonal Slater-Koster tight-binding Hamiltonian to evaluate the electron-phonon matrix elements. The results showed that the soft phonon near $Q_0=(\frac{2}{3},\frac{2}{3},0)\pi/a$, which results in a premartensitic phase transition in the β-phase NiTi alloy, was due to the strong electron-phonon coupling of the nested electronic states on the Fermi surface. The martensitic transformation in NiTi alloys and the resulting changes in optical properties will be the subject of a future publication.[27]

The dielectric functions of all three compounds were measured by spectroscopic ellipsometry[14–16] in the energy range of 0.062 to 4.96 eV. The measured optical spectra showed a close resemblance to each other above 1.5 eV, while there are large differences below 1.5 eV. Sasovskaya[16] ascribed the structures in the measured optical conductivity spectra above 1 eV to interband transitions between the two d bands separated by the deep minimum near the Fermi level. Sasovskaya[16] compared the experimental spectra to the calculated ones,[28] in which the interband transition matrix elements are assumed to be constant. Since the calculated optical conductivity spectra did not reproduce well the measured ones, Sasovskaya concluded that the theoretical models of the band structure of these compounds needed to be improved. However, the calculation[28] did not include the opti-

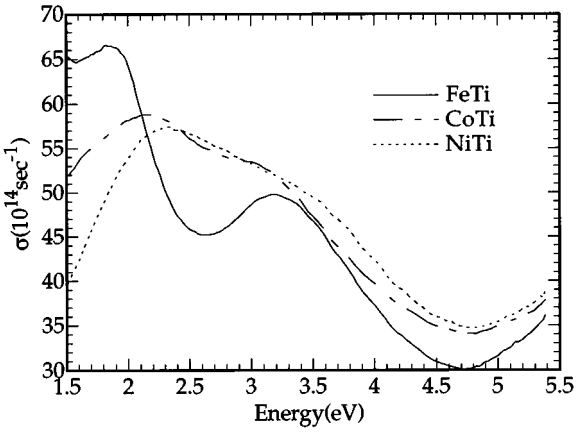

FIG. 1. The optical conductivity spectra of $B2$ phase FeTi, CoTi, and NiTi alloys. Note that the zero of the optical conductivity is suppressed.

cal transition matrix elements which are important for an accurate calculation of the optical conductivity. The inclusion of the optical matrix elements frequently results in an important modification to theoretical spectra determined by simple joint-density-of-states calculations.[29]

In this work we report the results of new measurements of the dielectric functions of the three compounds using spectroscopic ellipsometry in the energy range of 1.5–5.4 eV. FeTi and CoTi were measured at room temperature and NiTi at ~150 °C. The measured spectra exhibited features similar to the previous measurements, but the magnitudes are different to some degree. We also report the band structures and the calculated optical conductivity spectra using the linearized-augmented-plane-wave (LAPW) method. In the course of the optical conductivity calculations we included the dipole transition matrix elements. By employing a simple approximation for self-energy corrections we were able to generate calculated spectra qualitatively close to the measured ones.

The alloy samples were prepared by electron-beam melting in vacuum by the Materials Preparation Center of the Ames Laboratory. The starting elements were all of 99.99% purity or greater. The ingots were remelted several times to promote homogeneity. The weight lost during melting indicated that the samples were within 1% of the 50-50 composition intended. They were cut by a low-speed diamond saw into thin slabs for optical measurements. The slabs were mechanically polished with a series of alumina powders down to 0.05 μm diameter, then cleaned with acetone and methanol using an ultrasonic cleaner. We did not electropolish the sample. The polished and cleaned samples were annealed in ultrahigh vacuum because we found that annealing increases the magnitude of the optical conductivity. We used a spectroscopic rotating-analyzer ellipsometer, described in detail elsewhere,[30] for the measurement of the dielectric functions.

The measured optical conductivity spectra of the three compounds are shown in Fig. 1. The overall shapes of the spectra are qualitatively similar to previous measurements,[14–16] however, there are differences in some aspects. All spectra have broad two-peak features but the fine structures observed in the previous measurements were not observed, especially for NiTi (Ref. 14) and FeTi.[15]

The magnitudes of the optical conductivity at 2 eV are 16% larger for NiTi, 8.5% larger for CoTi, and 5% smaller for FeTi, than previously reported spectra. The samples used for the previous measurements were electropolished. Electropolishing leaves a chemical overlayer and wavy surface because of the nonuniform removal of the surface layer during electropolishing. Although both the surface roughness and a chemical overlayer are known to reduce the magnitude of the optical conductivity,[29–32] we cannot draw any definite conclusion for now because our measurements give just a slightly larger optical conductivity for CoTi, but a smaller one for FeTi.

The low-energy peak moves toward lower energy from NiTi to FeTi. For NiTi it is located around 2.3 eV and for CoTi around 2.2 eV. For CoTi there is a very weak shoulder around 1.7 eV, which may be an indication of splitting of the 2.3 eV peak of NiTi. Only a single peak at 1.86 eV was observed for FeTi, while the optical conductivity spectrum of Ref. 15 has two peaks located at 1.3 and 1.8 eV. Although we did not observe the splitting since the 1.3 eV peak is out of the spectral range of our ellipsometer, our FeTi spectrum shows decreasing optical conductivity below 1.8 eV as energy decreases and an upturn below 1.6 eV, having a local minimum around 1.6 eV.

The evolution of the two peaks, particularly the low-energy peak, was clearly exhibited in the optical conductivity spectra of pseudobinary $Fe_{1-x}Co_xTi$ alloys.[17] The lower peak (denoted as peak A at 1.3 eV in Refs. 16 and 17) did not appear in the optical conductivity spectra for $x=1.0$, 0.8, and 0.7 and the higher peak (denoted as peak B) moves from 2.2 eV (for $x=1.0$) to 1.9 eV (for $x=0.7$). For $x=0.3$ there appears a weak shoulder around 1.4 eV and it is enhanced and becomes a peak at 1.3 eV for $x=0.2$. For $x=0.0$ (FeTi) the two peaks have almost the same intensity.[15] The evolution of the low-energy peaks, which have a very strong dependence on concentration, was explained by using the rigid-band model. In other words, the shift of the Fermi level relative to the fixed DOS and energy band curves is proposed as being responsible for the evolution of the low-energy peak.[16,17] However our calculations reveal a somewhat different picture (see below).

The high-energy structure, denoted as peak D in Ref. 16, changes less than the low-energy one. It is located at 3.1 eV for CoTi, 3.2 eV for FeTi, and 3.4 eV for NiTi. This structure becomes more prominent from NiTi to FeTi. It is only a shoulder for NiTi and becomes clearly a peak for CoTi. For FeTi it is separated from the low-energy peak with a deep minimum around 2.6 eV. This kind of concentration dependence of the high-energy peak was also observed in $Fe_{1-x}Co_xTi$ alloys.[17]

To understand the similarities and the differences among the optical conductivity spectra of the three compounds we performed band structure and optical conductivity calculations in the $B2$ phase using the LAPW method.[33] The standard muffin-tin approximation for the potential was used, as was the local density approximation for the exchange-correlation potential.[34] The spin-orbit coupling was included in the self-consistent calculation. The spin-orbit Hamiltonian was diagonalized after the scalar-relativistic bands and wave functions had been obtained.[33] The parameters used in the band structure calculations, such as lattice constants and

TABLE I. Parameters used in the calculations.

	FeTi	CoTi	NiTi
Lattice constants	5.6238 a.u.	5.6597 a.u.	5.6994 a.u.
R_{MT}[a] for X	2.3265 a.u.	2.4003 a.u.	2.4003 a.u.
R_{MT} for Ti	2.4765 a.u.	2.4765 a.u.	2.4765 a.u.
Self-energy correction factor			
λ[b]	−0.18	−0.18	−0.20

[a]Muffin-tin radius.

[b]$\sigma_c(\omega)=1/(1+\lambda)\,\sigma_u[\omega/(1+\lambda)]$, where ''$c$'' and ''$u$'' stand for ''corrected'' and ''uncorrected,'' respectively.

muffin-tin radii, are listed in Table I. The lattice constants were taken from Ref. 35. About 150 to 160 LAPW basis functions, depending on the **k** point, were used. The energy eigenvalues at 120 **k** points in the irreducible Brillouin zone [IBZ=$\frac{1}{48}$ of the whole Brillouin zone (BZ)] were calculated for each self-consistent iteration.

Once the self-consistent potential and the charge density were obtained, we calculated the DOS and the optical conductivity spectra using the linear-tetrahedron method[36] and direct interband transition matrix elements. 512 tetrahedra in the IBZ, corresponding to 24 576 tetrahedra in the whole BZ, were used in the DOS and optical conductivity calculations. An approximation for the quasiparticle self-energy was included by the method described elsewhere.[29,37] The parameters for the self-energy correction are also listed in Table I.

The calculated band structures along the high-symmetry lines are shown in Figs. 2, 3, and 4 for FeTi, CoTi, and NiTi, respectively. The calculated band structures of FeTi, CoTi, and NiTi are very similar to those of Ref. 22, Ref. 20, and Ref. 25, respectively. Additionally, as mentioned in Ref. 20, the band structure of the three compounds are qualitatively similar to each other. The band structures of NiTi and CoTi are nearly identical, except for the position of the Fermi level. FeTi has a somewhat different band structure from the others, especially the order of the bands at the X point and along the $\Gamma-M$ line.

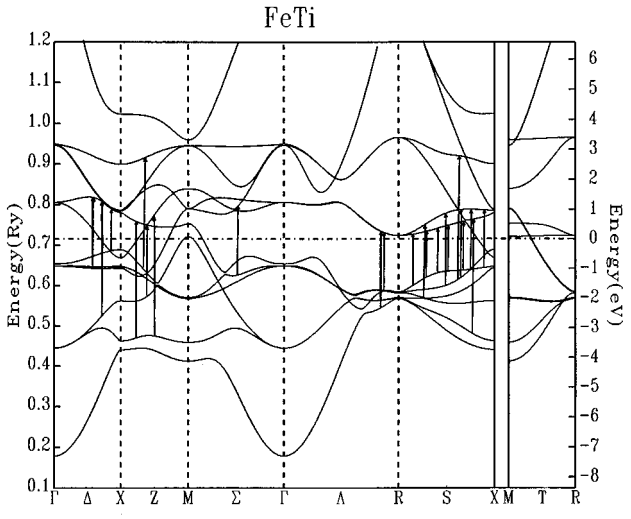

FIG. 2. Band structure of FeTi in the $B2$ phase along high-symmetry lines. Strong direct interband transitions corresponding to the measured peaks are denoted by the arrows.

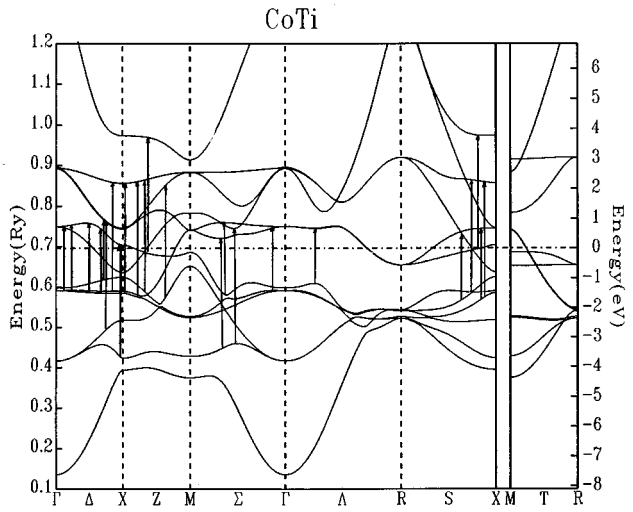

FIG. 3. The same as for Fig. 2, except for CoTi.

At the X point, band 7 is close to band 8 and about 1 eV higher than band 6 for NiTi. It is separated from band 8 and comes close to band 6 for CoTi and there is a reversal of bands 6 and 7 for FeTi. For CoTi the energy difference between bands 6 and 7 is about 0.2 eV. Band 8 also moves upwards from NiTi to FeTi. It is occupied and separated from bands 9 and 10 for NiTi, while it is unoccupied and located midway between band 7 and bands 9 and 10 for CoTi. For FeTi band 8 moves even higher to touch bands 9 and 10.

On the $\Gamma-M$ line, bands 7, 8, and 9 cross each other around the midpoint of the $\Gamma-M$ line and they are located above the Fermi level for FeTi. For CoTi band 7 moves downward and only bands 8 and 9 cross each other. On the other hand, the three bands never cross each other for NiTi and band 7 even touches the Fermi level at about 3/4 way from the Γ point.

The calculated DOS curves (Fig. 5) are almost the same as those of Ref. 20. The DOS curves have two main peaks, separated by a deep minimum around the Fermi level. The

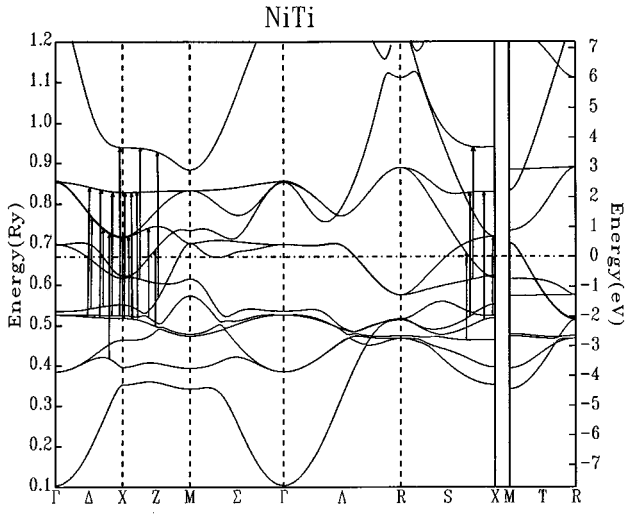

FIG. 4. The same as for Fig. 2, except for NiTi.

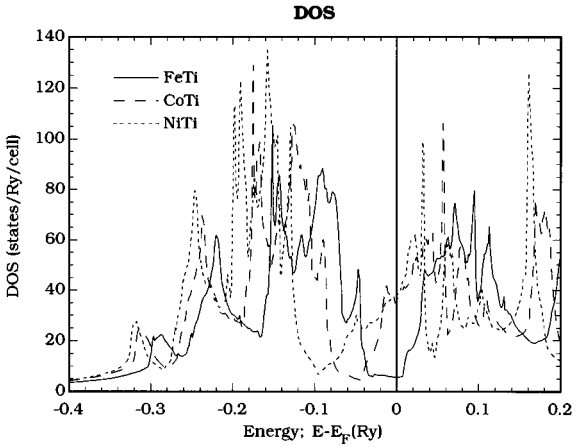

FIG. 5. The DOS curves of FeTi (solid line), CoTi (long dashed line), and NiTi (short dashed line).

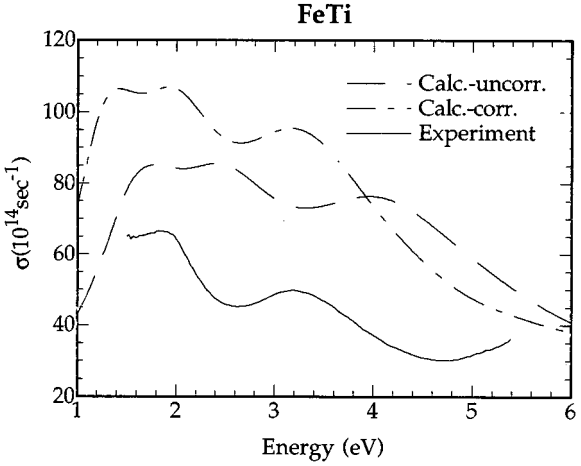

FIG. 6. The calculated (broadened) optical conductivity spectra of $B2$ phase FeTi, with (dashed curve) and without (dotted curve) the self-energy correction. The experimental one is also shown (solid curve). Note that the zero of the optical conductivity is suppressed.

angular momentum decomposed, partial DOS curves show that the characteristics of the two bands are the same as those of Ref. 20. The lower band is composed of mainly Fe, Co, or Ni d character, while the higher band is dominated by Ti d character. For FeTi the DOS curve has a flat and deep minimum near the Fermi level with a width of 0.56 eV and the Fermi level is located at the rising point of the flat minimum on the high-energy side of the DOS curve. The minimum separates the bonding and antibonding states. The width of the flat minimum decreases and becomes a sharp minimum as the electronic concentration increases. As shown in Ref. 20 the width of the lower bands (bonding states) decreases from FeTi to NiTi, while that of the upper bands (antibonding states) increases.

The greatest stability and the strongest covalency of FeTi in the $B2$ phase among the three transition-metal titanides can be explained by the location of the Fermi level.[20,21] It is known[21] that the intermetallic compounds of transition metals form very stable ordered CsCl structure when the average number of conduction electrons (including d electrons) is equal to six electrons/atom and the DOS curve has a deep minimum separating bonding and antibonding states where the Fermi level is located. FeTi has six conduction electrons per atom and the Fermi level falls in the deep minimum of the DOS curve.

The Fermi level moves almost 1 eV toward higher energy from FeTi to NiTi because the increased electronic concentration starts to fill the antibonding states. The Fermi level is located around the first sharp maximum of the antibonding states for NiTi in Ref. 20, while our calculation does not show any DOS peak at the Fermi level. Rather it is located at a weak shoulder, which rises to the second maximum in the antibonding states. Sasovskaya[15] argued that this fact appears to determine the instability of the $B2$ phase for NiTi at room temperature, because it is shown[38] that, for compounds possessing the $A15$ (β-tungsten) crystal structure, a DOS peak near the Fermi level is responsible for their structural instability. We suspect that initial instability is rather due to the Fermi surface nesting feature rather than from a peak in the DOS curve. The Fermi level of CoTi falls on the first shallow minimum of the DOS curve, and this location of the Fermi level of CoTi appears to determine the relative stability of the $B2$ phase at room temperature.

The DOS at the Fermi level for the compounds are 0.21 (FeTi), 1.33 (CoTi), and 1.41 (NiTi) in units of *states/spin/eV/unit cell*, which are comparable to the experimental values of 0.19 for FeTi,[3] 1.66 for CoTi,[3] and 1.73 for NiTi.[7] The calculated values are also comparable to those of the previous calculations.[20] The experimental values are obtained from magnetic susceptibility measurements.

Usually calculated optical conductivity spectra have many sharp peaks and fine structures which can hardly be observed in measurements. Those sharp structures are not observable since the calculations are usually done for the zero-temperature ground state ignoring lifetime dependent broadening. Also the instrumental resolution smears out many fine features. To simulate these effects we used Lorentzian lifetime broadening with an energy-dependent broadening factor.[39]

The calculated optical conductivity spectra are compared with the corresponding experimental spectra in Figs. 6, 7, and 8 for FeTi, CoTi, and NiTi, respectively. The broadened spectra produce shapes similar to the measured ones for all three compounds with the theoretical peaks occurring at higher energies than the measured ones. This is usual for transition metals[37,40] and their intermetallic compounds.[29] It is believed to be due to the reduced energy of low-lying excited states near the Fermi level relative to the energy calculated from the ground state potential.[37] The effect motivated the consideration of an approximate self-energy correction procedure explained elsewhere.[29,37] By applying this single parameter self-energy correction we are able to produce spectra with the peaks located at the same energies as the measured ones. The fitting parameters, λ, used here are listed in Table I. The numbers are typical for 3d transition metals and their intermetallic compounds; for example $\lambda = -0.18$ for Ni_3Al (Ref. 29) and $\lambda = -0.12$ for Ni.[40]

Except for the broadening and self-energy correction there are no adjustable or empirical parameters to make the theoretical spectra coincide with the measured ones. The

broadening and self-energy correction are optimized to give calculated spectra which agree with the measured ones around the lower-energy peaks.

Bremsstrahlung isochromat measurements on NiTi (Ref. 41) gave evidence for an electronic charge transfer from Ti to Ni spheres on alloying Ti with Ni. The calculated DOS reproduces the Bremsstrahlung isochromat spectrum with the peaks at lower energy than the calculation and, therefore, the Ti *d* band approximately 4 eV above the Fermi level in the calculated DOS curve should be relocated closer to the Fermi level. Photoelectron spectroscopy of FeTi (Ref. 10) also shows that the features of the photoelectron energy distribution appear ~ 0.25 eV to lower binding energy than the theory predicted. The negative sign of λ is consistent with these two experimental observations. The author of Ref. 16 also argued that, since the positions of the upper and lower *d* bands of the DOS curve were inaccurately located and both should be contracted toward the Fermi level, the calculated optical conductivity spectrum should be closer to the experiment, even though the calculation of Ref. 16 did not include optical matrix elements.

In the measured spectra we did not see the fine structures observed in the previous measurements, such as a 2.6 eV peak of NiTi (Ref. 14) and the double-peak structure on the high-energy peak of FeTi around 3.2 eV.[15] We do not fully understand the reason for the discrepancy in the measurements regarding the previously reported fine structure. However, our calculated spectra also do not show such fine structures, even before broadening.

For understanding of the evolution of the peaks from NiTi to FeTi and the splitting of the low-energy peak, we compiled information on the **k** points and bands contributing significantly to the optical conductivity. This information along the high-symmetry lines is shown in Figs. 2, 3, and 4 where the main interband transitions for the two peaks are denoted by arrows.

For the low-energy peak of NiTi, the most prominent contributions are from **k** points on the middle portion of the $\Gamma-X-M$ line and near it. Although quite a wide range of low-symmetry **k** points inside the Brillouin zone also contribute to the peak, those **k** points have much smaller transition matrix elements. Therefore we are considering only the transitions near the high-symmetry **k** points. The bands involved in those transitions are bands 4, 5, and 6 (mainly Ni *d* character) for the initial states and bands 9 and 10 (mainly Ti *d* character) for the final states. For the high-energy peak the main contributions come from almost the same **k** points as the low-energy peak with transitions from bands 4 and 5 to band 11, from band 2 to the 9 or from band 7 to band 12. Band 2 has 82% Ni *d* character and 18% Ti *d* character at the midpoint of the $\Gamma-X$ line. A small contribution comes from the **k** points near the *X* point on the $R-X$ line. The bands involved are the same as the previous ones. It should be noted that the transitions from the Ni *d* band below E_F to the Ti *d* band above E_F are allowed because the Ti *d* orbitals extend into the Ni sphere with $l=1$ or 3 character.

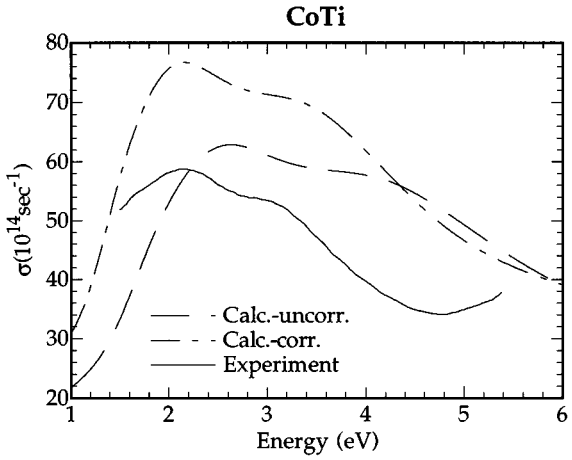

FIG. 7. The same as for Fig. 6, except for CoTi.

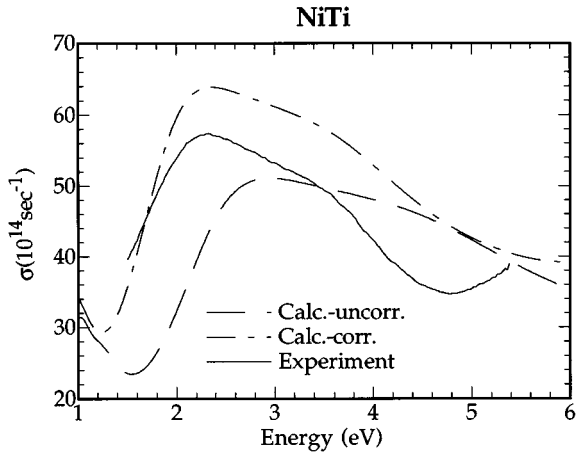

FIG. 8. The same as for Fig. 6, except for NiTi.

In Ref. 14 the bands and **k**-point assignments for the low-energy peak of NiTi are quite different from ours. However, since the calculation of Ref. 14 did not include the optical matrix elements, those assignments must be considered as tentative. Assignments, such as $X_3-X_{5'}$ (2.16 eV) and $X_5-X_{5'}$ (2.7 eV) are the same as ours, however, our calculation did not show any appreciable contributions from the **k** points along the Σ direction for the low-energy peak.

For CoTi the situation is very similar to the case of NiTi. The most important contributions to both peaks come from the **k** points near the $\Gamma-X-M$ line and the $R-X$ line. For the low-energy peak the bands involved in the transitions are very similar to NiTi. However, the important contributions extend to the Γ point on the $\Gamma-X$ line and the bands involved in the high-energy peak are slightly different from those of NiTi. The transitions from band 3 to bands 7 and 8 and from band 5 to band 11 are the main contributions. Band characters are similar to those of NiTi.

Although FeTi and CoTi have very similar transition characteristics, the transitions at the **k** points on the $R-X$ line extend to the whole line and the final states are mainly Ti *d* character with an admixture of Ni *d* character for the low-energy peak of FeTi. For all three compounds the low-energy peak has similar transition characteristics, from bands 4, 5, and 6 to bands 9 and 10 on the $\Gamma-X-M$ line. However, this contribution decreases, while the contribution from the **k** points on the $R-X$ line increases from NiTi to FeTi. The bands along the $R-X$ line involved in the significant transitions are almost parallel and the transition energies near the $R-X$ line are slightly smaller than those along the

$\Gamma-X-M$ line. Hence, the optical conductivity of the lower-energy side on the low-energy peak is enhanced as the electronic concentration decreases, i.e., from NiTi to FeTi, resulting in a two-peak structure of the low-energy peak of FeTi. This splitting is also enhanced by the fact that band 6 around the X point is raised to higher energy from NiTi to CoTi and band reversal occurs in FeTi. For CoTi and NiTi band 7 on the $R-X$ line, corresponding to the final states of the transition for the low-energy peak of FeTi, is mostly occupied and, hence, does not contribute to the optical conductivity.

In the measured energy range the calculated optical conductivity spectrum of FeTi has almost 40% and 50% larger magnitude than CoTi and NiTi, respectively, in the region below 2.5 eV. The larger magnitude is due to the effect of the joint density of states (JDOS) and/or the optical transition matrix elements. To determine which one dominates, we calculated the JDOS and analyzed the matrix elements. The calculated JDOS curves did not show any significant differences among the three compounds, except for the increased JDOS below 1.6 eV for FeTi because of the increased contributions from the $R-X$ line. Hence we concluded that the JDOS does not play a significant role to the larger optical conductivity of FeTi at low energy, except for below 1.6 eV. We compared the magnitude of the optical matrix elements of all three compounds and found that FeTi has significantly larger values for almost all **k** points than the other two compounds. Therefore the optical matrix elements give more prominent effects than JDOS for the larger optical conductivity of FeTi.

According to Ref. 16 the lack of dependence on the electronic concentration of the high-energy peak was explained by the fact that the high-energy peak is mainly due to transitions between the occupied part of the d band of the heavier component (Fe, Co, Ni) and the band of the zone boundaries (d states of Ti), which is a typical feature of the electronic spectrum of intermetallic compounds with the CsCl structure.[42–48] The energy differences between the occupied d band of the heavier component (Fe, Co, Ni) and the unoccupied Ti d band do not change appreciably as the electronic concentration increases, i.e., from FeTi to NiTi. Our calculation shows that the final states for the high-energy peak are mostly in band 11 for NiTi. Band 11 has predominantly Ti d character and is quite flat along many high-symmetry lines for all three compounds.

For NiTi the main contributions are due to the transitions between bands 4 and 5 and band 11 at **k** points on the $\Gamma-X-M$ line and near it. As mentioned in the discussion of the DOS, the initial states have mainly Ni d character with an admixture of Ti d character and the final states have mainly Ti d character for NiTi. The characteristics of the bands involved in the transition for the high-energy peak are altered in CoTi. The transitions from band 7 to band 12 decrease in CoTi. FeTi has similar transition characteristics to CoTi. However, the contributions from band 11 as a final state are significantly reduced.

This alteration of bands involved in the transition can explain the slight decrease in energy of the high-energy peak from NiTi to FeTi. Since the initial state moves to higher energy and the final state moves to lower energy, the energy of the optical transition decreases slightly as the electronic concentration decreases.

The angular-momentum-decomposed optical conductivity shows that a non-negligible contribution of $f\rightarrow d$ transitions exists in the Ti sphere. There is no unique way of angular-momentum decomposition of the optical conductivity, because of interference effects, which occur when the angular-momentum-decomposed complex optical transition matrix elements are added and squared. Therefore one should be cautious when trying to interpret the non-negligible $f\rightarrow d$ transitions in the Ti sphere. The calculations showed that, for all three compounds, the angular-momentum-decomposed valence-electron-charge (VEC) density has a small but non-negligible f character and the f character of the Ti sphere is almost twice as large as that of the Fe, Co, or Ni spheres. For FeTi, the Ti sphere has 0.04 f electrons and the Fe sphere has 0.02. These numbers are the same as those of Ref. 22. The larger f character in the Ti sphere than in the Fe, Co, or Ni spheres is due to the long tail of the Fe, Co, or Ni radial functions which extend into the Ti sphere and can have $l=3$ character there. Since the amount of f character is negligible, compared to the total VEC (six electrons per atom), it is rather striking that the $f\rightarrow d$ transitions in the Ti sphere are non-negligible. Detailed analysis of the $f\rightarrow d$ optical transition matrix elements shows that the radial-function integration has a comparable magnitude to the $d\rightarrow p$ and other main transitions, in spite of the small amount of f character in the whole wave function, making $f\rightarrow d$ contributions non-negligible.

In summary, we measured the optical conductivity spectra of equiatomic XTi (X=Fe, Co, and Ni) alloys in the $B2$ phase using spectroscopic ellipsometry. Although the measured spectra are qualitatively similar to the previous ones, our measurements are slightly different in magnitude and we did not observe fine structures as in the previously measured spectra. We used the LAPW method to calculate the band structures and optical conductivity spectra. The broadened and self-energy corrected optical conductivity spectra can reproduce reasonably the measured ones. The splitting of the low-energy peak of FeTi is due to increased optical transitions at the **k** points near the $R-X$ line, where the initial and final bands, whose energy differences correspond to the lower-energy side of the low-energy peak, are almost parallel to each other. The differences among the spectra of the three compounds can be explained by the different transition characteristics from different **k** points in BZ and different bands involved in the transitions.

One of the authors (J.Y.R.) wishes to thank Hoseo University for the financial support. The Ames Laboratory is operated for the U.S. Department of Energy by Iowa State University under Contract No. W-7405-Eng-82.

[1] G. M. Michal and R. Sinclair, Acta. Cryst. B **37**, 1803 (1981).
[2] F. E. Wang, W. J. Buehler, and S. J. Pickart, J. Appl. Phys. **36**, 3232 (1965).
[3] Y. Asada and H. Nose, J. Phys. Soc. Jpn. **35**, 409 (1973).
[4] G. Hilscher, N. Buis, and J. J. M. Franse, Physica **91B**, 170 (1977).
[5] J. Kübler, J. Magn. Magn. Mater. **15-18**, 859 (1980).
[6] G. Schadler and P. Weinberger, J. Phys. F **16**, 27 (1986).
[7] M. A. Mitchell, F. E. Wang, and J. R. Cullen, J. Appl. Phys. **45**, 3337 (1974).
[8] E. V. Mielczarek and W. Winfree, Phys. Rev. B **11**, 1026 (1975).
[9] N. Motta, M. de Crescenzi, and A. Balzarotti, Phys. Rev. B **27**, 4712 (1983).
[10] J. H. Weaver and D. T. Peterson, Phys. Rev. B **22**, 3624 (1980).
[11] J. C. Fuggle, F. U. Hillebrecht, R. Zeller, Z. Zolnierek, P. A. Bennet, and Ch. Freiburg, Phys. Rev. B **27**, 2145 (1983).
[12] E. A. Starke, C. H. Cheng, and P. A. Beck, Phys. Rev. **126**, 1746 (1962).
[13] R. S. Allgaier, J. Phys. Chem. Sol. **28**, 1293 (1967).
[14] I. I. Sasovskaya, S. A. Shabalovskaya, and A. I. Lotkov, Sov. Phys. JETP **50**, 1128 (1979).
[15] I. I. Sasovskaya, Phys. Met. Metall. **50**, 64 (1980).
[16] I. I. Sasovskaya, Phys. Met. Metall. **69**, 72 (1990).
[17] I. I. Sasovskaya, Phys. Status Solidi B **164**, 327 (1991).
[18] G. N. Kamm, Phys. Rev. B **12**, 3013 (1975).
[19] D. A. Papaconstantopoulos and D. J. Nagel, Int. J. Quantum Chem. **S5**, 515 (1971).
[20] R. Eibler, J. Redinger, and A. Neckel, J. Phys. F **17**, 1533 (1987).
[21] J. Yamashita and S. Asano, Prog. Theor. Phys. **48**, 2119 (1972).
[22] D. A. Papaconstantopoulos, Phys. Rev. B **11**, 4801 (1975).
[23] M. Šob, J. Phys. F **12**, 571 (1982).
[24] D. A. Papaconstantopoulos, G. N. Kamm, and P. N. Poulopoulos, Solid State Commun. **41**, 93 (1982).
[25] G. Bilhlmayer, R. Eibler, and A. Neckel, Ber. Bunsenges. Phys. Chem. **96**, 1626 (1992).
[26] G. L. Zhao and B. N. Harmon, Phys. Rev. B **48**, 2031 (1993).
[27] J. Y. Rhee, B. N. Harmon, and D. W. Lynch (unpublished).
[28] V. Y. Yegorushkin and N. I. Fedyaynova, *Alloys of Rare Metals with Special Physical Properties* (Nauka, Moscow, 1983), p. 24.
[29] J. Y. Rhee, B. N. Harmon, and D. W. Lynch (unpublished).
[30] J. Y. Rhee, Ph.D. Thesis, Iowa State University, 1992 (unpublished).
[31] D. E. Aspnes, E. Kinsbron, and D. D. Bacon, Phys. Rev. B **21**, 3290 (1980).
[32] T. Yasuda and D. E. Aspnes, Appl. Opt. **33**, 7435 (1994).
[33] D. D. Koelling and B. N. Harmon, J. Phys. C **10**, 3170 (1977); O. K. Andersen, Phys. Rev. B **12**, 3060 (1975).
[34] L. Hedin and B. I. Lundqvist, J. Phys. C **4**, 2064 (1971).
[35] P. Villars and L. D. Calvert, *Pearson's Handbook of Crystallographic Data for Intermetallic Phases* (American Society of Metals, Metals Park, 1985), Vol. 2.
[36] O. Jepsen and O. K. Andersen, Solid State Commun. **9**, 1763 (1971).
[37] J. F. Janak, A. R. Williams, and V. L. Moruzzi, Phys. Rev. B **11**, 1522 (1975).
[38] M. Weger and I. B. Goldberg, in *Solid State Physics*, edited by H. Ehrenreich, F. Seitz, and D. Turnbull (Academic, New York, 1973), Vol. 28, p. 1.
[39] An energy dependent Lorentzian broadening function of width $\Gamma(E)=AE^2/\mathrm{eV}$, where $E=[E_f(\mathbf{k})-E_i(\mathbf{k})]$ in eV, was used. We set the upper limit of $\Gamma(E)_{\max}=2$ eV for better agreement.
[40] D. G. Laurent, J. Callaway, and C. S. Wang, Phys. Rev. B **20**, 1134 (1979).
[41] H. Föll, Z. Phys. B **26**, 329 (1977).
[42] V. L. Moruzzi, A. R. Williams, and J. F. Janak, Phys. Rev. B **10**, 4856 (1974).
[43] S. A. Nemnonv and K. M. Kolobova, Phys. Met. Metall. **23**, 66 (1967).
[44] J. R. Cuthill, A. J. McAlister, and M. L. Williams, J. Appl. Phys. **39**, 2204 (1968).
[45] K. M. Kolobova and V. A. Trofinova, in *Proceedings of the International Symposium, Kiev, 1968* (Inst. Met. Phys. Acad. Sci. Ukr, SSR, 1968), p. 179.
[46] J. E. Holliday, J. Phys. Chem. Solids **32**, 1825 (1971).
[47] E. Källne, J. Phys. F **4**, 167 (1974).
[48] T. K. Boletskaya, V. E. Egorushkin, E. M. Savitskii, and V. P. Fadin, Dokl. Acad. Nauk **252**, 87 (1980).